Published in final edited form as:
J Immunol. 2009 June 1; 182(11): 7009–7018. doi:10.4049/jimmunol.0804031.

The Binding of Factor H to a Complex of Physiological Polyanions and C3b on Cells is Impaired in Atypical Hemolytic Uremic Syndrome[1]

Viviana P. Ferreira[*], **Andrew P. Herbert**[†], **Claudio Cortés**[*], **Kristi A. McKee**[*], **Bärbel S. Blaum**[†], **Stefan T. Esswein**[†], **Dušan Uhrín**[†], **Paul N. Barlow**[†], **Michael K. Pangburn**[*], and **David Kavanagh**[†,2]

[*]Department of Biochemistry, Center for Biomedical Research, University of Texas Health Science Center, Tyler, TX. 75708

[†]Edinburgh Biomolecular NMR Unit, Schools of Chemistry and Biological Sciences, University of Edinburgh, Edinburgh, EH9 3JJ, United Kingdom.

Abstract

Factor H (fH) is essential for complement homeostasis in fluid-phase and on surfaces. Its two C-terminal domains (CCP 19-20) anchor fH to self surfaces where it prevents C3b amplification in a process requiring its N-terminal four domains. In atypical hemolytic uremic syndrome (aHUS), mutations clustering towards the C-terminus of fH may disrupt interactions with surface-associated C3b or polyanions and thereby diminish the ability of fH to regulate complement. To test this we compared a recombinant protein encompassing CCP 19-20 with sixteen mutants. The mutations had only very limited and localized effects on protein structure. While we found four aHUS-linked fH mutations that decreased binding to C3b and/or to heparin (a model compound for cell-surface polyanionic carbohydrates), we identified five aHUS-associated mutants with increased affinity for either or both ligands. Strikingly, these variable affinities for the individual ligands did not correlate with the extent to which all the aHUS-associated mutants were found to be impaired in a more physiological assay that measured their ability to inhibit cell surface complement functions of full-length fH. Taken together, our data suggest that disruption of a complex fH-self surface recognition process, involving a balance of affinities for protein and physiological carbohydrate ligands, predisposes to aHUS.

[1]This research was supported by American Heart Association National Scientist Development Grant 0735101N (V.F.), D.K. is a Kidney Research UK Clinical Training Fellow, National Institutes of Health Grant DK-35081 (M.K.P.), Wellcome Trust Grant 078780/Z/05/Z (D.U. and P.N.B.).

[2]Address correspondence and reprint requests to Dr. David Kavanagh, Edinburgh Biomolecular NMR Unit, Schools of Chemistry and Biological Sciences, Joseph Black Chemistry Bldg., University of Edinburgh, West Mains Rd., Edinburgh EH9 3JJ, United Kingdom. Email: davidkavanagh@doctors.org.uk; Telephone: +44(0)191-244-8274; Fax: +44(0)191-284-9845.

Disclosure

One of the authors (M.K.P.) is an officer of and has a financial interest in Complement Technology, Inc. (www.ComplementTech.com), a supplier of complement reagents.

Europe PMC Funders Author Manuscripts

Keywords

Complement; Human; Cell Surface Molecules

Europe PMC Funders Author Manuscripts

Introduction

Atypical hemolytic uremic syndrome (aHUS) is a disease characterized by hemolytic anemia, thrombocytopenia and acute renal failure (1). In 1998, Warwicker *et al.* described mutations in the complement regulator, factor H (fH), associated with aHUS (2). This observation was subsequently confirmed in five independent cohorts of aHUS patients (3-7). The majority of these mutations are heterozygous and cluster in the C-terminus of fH. Incomplete penetrance is described in all reports, suggesting that a combination of mutations, risk haplotypes, and precipitating factors, such as infection or pregnancy, are required for aHUS to manifest (8-12).

Factor H, an abundant serum glycoprotein (~500 μg/ml), plays a key role in the homeostasis of the complement system. It accelerates the decay of C3b,Bb complexes that, in the alternative pathway, proteolytically convert C3 to its activated form, C3b (13). It is also a cofactor for factor I-mediated cleavage and inactivation of C3b (14). Factor H is composed of 20 complement control protein modules (CCPs) that resemble beads on a flexible string in the transmission electron microscope (15, 16). The N-terminal four CCPs (*i.e.* CCP 1-4) encompass the region capable of cofactor and decay accelerating activity (17-20). A second principal C3b-binding site lies within the C-terminal pair of CCPs (CCP 19-20) and also interacts with iC3b and C3d (18, 21-23). At least two sites on fH (*i.e.* CCP 7 and CCP 20) interact with heparin and other polyanions (24-30). The C-terminal site additionally binds sialic acids (24, 28).

In the absence of fH, spontaneous activation of the alternative pathway of complement occurs in plasma, which leads to consumption of complement components C3 and factor B. In addition to its function as a regulator of alternative pathway activation in fluid phase, fH is essential for complement control on many self-surfaces. For example, it binds to human endothelial cells and basement membranes (31) protecting them from complement-mediated attack (32). Indeed, fH has a ten-fold higher affinity for C3b on host cells and other non-activators of complement *versus* activators, which is dependent on the presence of sialic acid clusters or other polyanions on the surface (33, 34). The specific chemical nature of human host markers has not been identified, but it is assumed to be polyanionic since sheep cells, which do not activate complement, activate the alternative pathway after surface sialic acid is removed (33, 34). Previous studies have shown that the C3b- and polyanion-binding sites in CCPs 19-20 are key for fH interactions with host surfaces (21, 22, 28, 31, 35-37). Furthermore, a recombinant form of these C-terminal CCPs (rH19-20) has been shown to compete with full-length fH for binding to C3b and host polyanions (35). This competition results in increased complement activation on host surfaces, without affecting control of complement in plasma (35).

The C-terminal module of fH is the most commonly mutated one in individuals with aHUS and functional analysis to date has demonstrated an associated impairment of binding to C3b and/or GAGs (38). Moreover, a transgenic mouse line expressing fH missing its C-terminal region regulated C3 activation in plasma but spontaneously developed aHUS (39). The truncated murine fH failed to bind to endothelial cells. Thus, in aHUS, the mutant form of fH is believed to regulate the alternative pathway of complement in the fluid phase, but fails to be recruited by glomerular endothelial cells and/or the glomerular basement membrane.

Controversy has arisen over the interpretation of the limited structure-function studies that attempted to assign disease-linked mutations in the fH C-terminus to binding sites on the fH C-terminus for specific ligands. Jokiranta *et al.* (40) concluded that aHUS-linked mutations lie in a C3d/b-binding site while the polyanion-binding site is not affected. On the other hand, Herbert *et al.* (41) presented evidence that shows that mutations cluster within an electropositive polyanion-binding site. Moreover, none of the disease-linked mutants have been analyzed with respect to their structural integrity; thus it remains possible that the mutations are destabilizing or result in unfolded protein. In the current work we set out to resolve these issues and to thereby address the question: why do aHUS-linked mutations prevent fH from functioning properly?

To avoid difficult-to-interpret complications likely to arise from the presence of additional C3b- and heparin-binding sites that reside within the N-terminal 18 CCPs of fH, we mutated and analyzed a recombinant construct containing only the CCPs 19 and 20 (rH19-20). We measured the affinity of each of sixteen rH19-20 mutants for C3b and, separately, for polyanions. Because C3b and host polyanions reside together on surfaces, we also used assays designed to measure the interactions with these ligands simultaneously in a physiological setting on the cell surface.

Materials and Methods

Red blood cells and buffers

Blood from sheep and from two healthy human adults was collected by venipuncture and the red cells were frozen at −80°C (42). The University of Texas Health Science Center institutional review board approved protocols, and written informed consent was obtained from all human donors. The buffers used were: PBS (10 mM sodium phosphate, 140 mM NaCl, 0.02% NaN_3, pH 7.4); veronal buffered saline (VBS), 5 mM veronal, 145 mM NaCl, 0.02% NaN_3, pH 7.3; GVB, VBS containing 0.1% gelatin; GVBE, GVB containing 10 mM ethylenediaminetetraacetic acid (EDTA); DGVB, half-physiological ionic-strength buffer prepared by diluting GVB two-fold with 5% dextrose in water; MgEGTA, 0.1 M $MgCl_2$, 0.1 M EGTA (ethyleneglycoltetraacetic acid), pH 7.3.

Purified proteins

Complement proteins fH (43), C3 (44, 45), factor B (46), and factor D (47) were purified from normal human plasma as described. A fragment consisting of C-terminal residues 1107-1231 of fH (domains 19-20, *i.e.* rH19-20) was cloned, expressed and purified as described (41). Site directed mutagenesis was used to generate sixteen mutant versions of rH19-20, using the Quickchange^R mutagenesis system (Stratagene, Cedar Creek, TX). Ten of these are associated with aHUS (D1119G, R1182S, W1183R, T1184R, L1189F, L1189R, S1191L, R1210C, R1215G, and double mutant S1191L;V1197A) (48); the remaining six mutants (E1172R, K1188Q, R1203S, R1203Y, R1210S, and K1230A) have not so far been observed in aHUS patients, but were generated to probe C3b- and polyanion-binding sites. The residues chosen for the design of these mutants lie in putative C3b- and polyanion-binding sites (40, 41) and cover a wider surface region within domain 20, which is where most aHUS-associated mutations in fH lie. The proteins were cloned and expressed using the *Pichia pastoris* strain KM71H as previously described (41). Mass spectra of recombinant proteins (purified by cation-exchange chromatography and stored at −80°C in PBS as described previously (41)) were consistent with predicted molecular weights. A ^{15}N-labelled sample of each mutant was prepared by using $(^{15}NH_4)_2SO_4$ (Isotec) as the sole source of nitrogen during cell growth. Protein concentrations were determined (280 nm) using theoretical $E^{1\%}_{1\ cm}$ values (49). Factor H and an aliquot of wildtype rH19-20 (100 μg) were radiolabeled with ^{125}I to specific activities of 4 to 6 μCi/μg as described (35).

Nuclear magnetic resonance (NMR) methods

For NMR, samples of ^{15}N labeled proteins were 100 μM in 20 mM deuterated sodium acetate, 10% D_2O, pH 4.5. In each case a [^{15}N,^{1}H] heteronuclear single quantum coherence (HSQC) spectrum was collected at 37°C on a Bruker AVANCE 800 MHz spectrometer fitted with a 5 mm CPDCI cryoprobe with Z gradients. Based on existing spectral assignments for wild type rH19-20 (41), analyses were conducted to reveal any changes in the ^{15}N and ^{1}H chemical shifts of each backbone amide consequent upon mutagenesis.

Heparin affinity chromatography

Protein samples (3 μM, 1 ml) in 20 mM potassium phosphate buffer, pH 7.4, at 20°C, were loaded individually onto a HiTrap heparin-affinity chromatography column (7 mm × 25 mm, GE Healthcare, Piscataway, NJ), equilibrated with the same buffer, and subsequently eluted with a 20-column volume gradient from 0–1 M NaCl in 20 mM potassium phosphate buffer, pH 7.4. Protein elution was monitored using absorbance at 280 nm. Similar experiments were carried out for the aHUS-associated mutants (0.6 μM, 5 ml) in 20 mM HEPES, pH 7.0, at 4°C, and eluted with a 20 column volume gradient from 0-1 M NaCl in 20 mM HEPES, pH 7.0.

Gel-mobility shift assays (GMSA)

Oligosaccharides were prepared for GMSA from low-molecular weight heparin by partial digestion with heparinase I followed by size-fractionation on a BioGel P10 gel-filtration column (BioRad, Hercules, CA) (50). In the case of the tetrasaccharide, dp4, strong anion-exchange chromatography (AS-17 Ionpac, Dionex, Sunnyvale, CA) was subsequently performed to isolate only fully sulfated product (ΔUA2S-GlcNS6S-IdoA2S-GlcNS6S). Due to the heterogeneity associated with the length of the hexasaccharide (dp6) this purification step was omitted in dp6 preparations resulting in variable sulfation patterns. Fluorophore-labeled species were produced by attachment of 2-aminoacridone to the oligosaccharide reducing end (50), and GMSAs were performed, as described previously (51).

Analysis of C3b binding by surface plasmon resonance (SPR)

A BIAcore 3000 instrument was used to perform SPR. Human C3b (800-2000 response units (RU)) was amine coupled to a CM5 sensor chip (GE Healthcare). In addition, a streptavidin (SA) sensor chip (GE Healthcare) was coated with biotinylated C3b, generated as recently described (52). For each type of sensor chip, three flow cells (Fc2, Fc3 and Fc4) were independently coupled with C3b. Then 20 μl injections of the rH19-20 mutants and wildtype rH19-20 were performed at 0-12 μM over the flow cells at 5 μl/min, at 22°C. The running and sample buffer consisted of PBS with 0.005% Tween. The maximum equilibrium binding of the proteins to C3b was measured by subtracting RUs obtained for the reference cell (Fc1) from the C3b-coupled flow cell RUs. The equilibrium binding values for each concentration were plotted using the Grafit 5 program (Erithacus), which determined the apparent K_d by fitting the data to a single-site saturation curve. Since the wildtype rH19-20 interacts with C3b with a 1:1 stoichiometry, the K_d values of the mutant proteins were calculated by setting the capacity (as a constant) to that of the average (n=12) capacity of wildtype rH19-20, for each C3b-coupled sensor chip.

Preparation of C3b-coated cells and zymosan particles—Deposition of C3b on sheep erythrocytes (E_S), and zymosan particles (Sigma-Aldrich, St. Louis, MO) was accomplished using purified C3, factor B and factor D as previously described (53). The number of bound C3b molecules was determined to be 125,000 per E_s cell or 100,000 per zymosan particle by measuring binding of radiolabeled factor Bb (53).

Binding assays with C3b-coated cells and zymosan

Sheep erythrocytes (E_SC3b) bearing a total of 1 μg C3b were incubated with ~20 ng of radioiodinated human fH and 0 to 8 μM non-labeled rH19-20 (wildtype or mutants) in 100 μl half-ionic strength buffer (DGVB). Alternatively, the cells were incubated with ~20 ng ^{125}I-rH19-20 and the non-labeled proteins. After 20 min at 22°C, the bound and free radiolabeled proteins were separated as described (34). The competition experiments with C3b-coated zymosan (ZymC3b) were carried out as described above, except only the IC_{50} dose of the unlabeled wildtype rH19-20 (1 μM) was compared to a 1 μM dose of various rH19-20 mutants.

Hemolysis assays

Lysis of human erythrocytes (35) (E_H) was measured by pre-incubating 5×10^6 E_H with 7 μg/ml anti-CD59 monoclonal antibody (clone MEM43; Abcam, Cambridge, MA) for 20 min at 4°C, and then mixing, on ice, with GVB, normal human serum (NHS; 40% final), and 0.1 M MgEGTA (5 mM final concentration) in the presence of 1 μM wildtype or mutant rH19-20. This concentration of wildtype rH19-20 is enough to achieve ~50% hemolysis (IC_{50}) of anti-CD59 treated cells, due to inhibition of fH-mediated protection. The mix was immediately transferred to a 37°C water bath and incubated for 20 min. To determine the extent of hemolysis induced by the mutants *versus* the wildtype rH19-20, 200 μl cold GVBE was added, the samples were centrifuged, and the optical density of the supernatant was determined at 414 nm. The percent lysis was determined by subtracting the A_{414} of the background lysis control, and dividing by the maximum lysis in water.

Statistical analysis

Conventional Student's *t* tests (2-tailed) were used to assess the statistical significance of the difference between wildtype rH19-20 and the mutants in their ability to bind to C3b (BIAcore), to C3b on zymosan, and to lyse E_H in the presence of NHS and p values <0.05 were considered statistically significant.

Results

A panel of mutant recombinant forms of fH domains 19-20 (rH19-20) was expressed in P. pastoris

A total of sixteen mutations of rH19-20 were expressed in *P. pastoris*, as summarized in Figure 1*A*. Ten of these correspond to aHUS-linked sequence variants (38). As previously noted (41) these, to a large extent, congregate on one face of module 20 (Fig. 1*A*). A further six mutants, that have not been identified in aHUS patients, but that cover a wider surface region of the disease-linked domain 20, were designed to help delineate binding sites for C3b and heparin. Based on previous studies (40, 41), the residues chosen for these "designer" mutants are hypothesized to lie within C3b- or polyanion-binding sites. All the mutants were homogeneous as judged by SDS-PAGE under both oxidizing and reducing conditions (not shown). The expected molecular weight of all the mutants was confirmed by electrospray ionization mass spectrometry (not shown).

The aHUS-linked mutations do not perturb structure

Samples of wildtype-sequence rH19-20, and of the mutant forms, were isotopically enriched with ^{15}N. Each sample was used to collect a 2D ^{15}N,^{1}H-HSQC spectrum. Nearly every amino acid residue within wildtype rH19-20 yielded a distinct peak in such a spectrum, as reported previously (41) and as expected for a properly folded polypeptide. For fifteen out of sixteen mutants, the ^{15}N,^{1}H-HSQC spectra (not shown) were also consistent with folded proteins; the exception was the designed mutant R1203Y, which was judged to be unfolded

by ^{1}H NMR. Furthermore, a comparison of HSQC spectra showed good conservation of chemical shifts with variations confined to the vicinity of the mutated residues. Moreover, lineshapes and spectral quality were consistent with monomeric protein for all proteins tested. These observations suggest that none of the aHUS-linked mutations resulted in major structural changes.

The aHUS-linked mutants bind with varying affinity to heparin

Previous work suggests that host GAGs form at least part of the target recognized by the C-terminal anchoring region of fH (25, 28, 31, 35, 37, 41). Thus it was of interest to assess the extent to which our mutations affect GAG binding. Heparin is commonly used as an experimental model compound for GAGs that are found on cell surfaces such as heparan sulfate and dermatan sulfate. The wildtype and mutant forms of rH19-20 were loaded onto a heparin-affinity column and eluted using a salt gradient (Fig. 2*A*-*B*). Some aHUS-linked mutants bound to the resin more tightly, others bound more weakly and the remainder eluted similarly to wildtype rH19-20. For example, the strongest interaction was found with W1183R (eluting at 520 mM NaCl), while the weakest was R1182S (eluting at 325 mM NaCl). The wildtype rH19-20 eluted at 370 mM NaCl. In general, mutations that resulted in gain of positive charge increased affinity (aHUS mutants W1183R, T1184R, L1189R; designed mutant E1172R), while mutations causing a loss of positive charge decreased affinity (aHUS mutants R1182S, R1210C, R1215G; designed mutants K1188Q, R1203A, R1210S, K1230A). To investigate further, GMSAs were performed. In these assays, the migration of a fluorescently tagged defined-length GAG fragment through an agarose gel was monitored in the presence of wildtype rH19-20 or the mutants. The wildtype protein binds and hence retards the mobility of both a chemically pure fully sulfated heparin-derived tetrasaccharide (dp4, data not shown), as well as heparin-derived hexasaccharides (dp6) that contain heterogeneous sulfation patterns (Fig. 2*C*). The experimental conditions were optimized so that the wild type showed some free dp6 migrating towards the anode. Smaller amounts of observed free dp6 for some mutants indicated stronger binding, while larger amounts corresponded to weaker binders. The ranking of affinities of rH19-20 mutants (aHUS-associated and designed mutants) for GAGs, as inferred from the GMSA (Fig. 2*C*), was very similar to the ranking derived from heparin-affinity chromatography (Fig. 2*A*-*B*). In summary, there is no uniform link between the affinity for heparin of the aHUS-associated mutants and aHUS pathology. Thus, some of the aHUS-associated mutants (W1183R, T1184R, L1189R, L1189F, S1191L, and S1191L;V1197A) were either unaffected or had increased affinity for heparin.

The aHUS-linked mutants bind with varying affinity to C3b

We measured the affinity of each mutant protein for C3b using SPR. C3b was immobilized on a CM5 sensor chip by amine coupling. Figure 3*A* summarizes the value of K_d obtained for each mutant. Four of the aHUS mutants (D1119G, R1182S, R1210C, and R1215G) bound with lower affinity to immobilized C3b, compared to the wildtype. The other aHUS mutants were either unaffected in their ability to bind (V1197A in the context of the S1191L;V1197A double mutant) or had a slightly (L1189F) or significantly (W1183R, T1184R, L1189R, S1191L) increased affinity for C3b. It is noteworthy that most of the aHUS mutants that clearly bind more strongly to C3b (*i.e.* W1183R, T1184R, L1189R) correspond to those with a higher affinity for heparin, while most of those with low affinity for C3b (*i.e.* R1182S, R1210C, R1215G) correspond to those exhibiting weaker heparin binding, as summarized in Figure 4. Interestingly, the aHUS mutant S1191L, which bound with greater affinity to C3b (Fig. 3-4), maintained a normal ability to bind heparin (Figs. 2 and 4).

A second type of sensor chip, pre-immobilized with streptavidin (SA chip), was used to immobilize C3b molecules that had been biotinylated at the cysteine-SH within the thioester site. This mode of immobilization emulates more closely the natural orientation of C3b on surfaces (52). Figure 3*C* shows representative equilibrium binding single-site saturation curves for rH19-20 wildtype as well as examples of a high-affinity (L1189R) and a low-affinity (R1215G) mutant binding to C3b. The K_d values obtained with the SA-C3b sensor chip (Fig. 3*B*) were very similar to those obtained on the CM5 chip (Fig. 3*A*). These findings indicate that the mode of C3b coupling did not bias the measured K_d values.

In order to further investigate the unexpected increase in affinity for C3b of some mutants as observed by SPR, C3b-coated zymosan particles (ZymC3b; which are devoid of polyanions) were incubated with radiolabeled wildtype rH19-20 in combination with unlabeled wildtype or the mutants with the highest and lowest affinity for C3b (by SPR). Figure 3*D* shows that aHUS mutants W1183R, T1184R, and L1189R as well as designed mutant E1172R, competed with radiolabeled rH19-20 more efficiently for binding to surface-bound native C3b than the unlabeled wildtype rH19-20, while aHUS mutants R1182S and D1119G were less efficient. The differences between the ability of the wildtype versus each of the mutants to bind to ZymC3b were all significant ($p<0.05$). These results agree with the SPR data, confirming that some disease-linked mutants do indeed bind with higher affinity to C3b. Taken together, the C3b-binding data show that there is no correlation between affinity for C3b and the association of the mutations with aHUS.

Delineating C3b and heparin binding sites

Considering our panel of sixteen rH19-20 mutations as a whole, fourteen neither introduced a cysteine (the exception being R1210C) nor resulted in structural disruption (the exception being R1203Y). Of these fourteen, nine had a positive or negative effect, compared to wildtype rH19-20, on both heparin and C3b binding, while one (V1197A, within the context of S1191L;V1197A double mutant) had no significant effect (Fig. 4). Two other mutations (R1210S and K1230A) decreased heparin binding, but did not alter C3b binding. Mutant D1119G significantly decreased C3b binding, but had no effect on heparin binding. On the other hand, S1191L increased C3b binding, while having no effect on heparin binding. Since these mutations resulted in only localized structural changes it seems valid to summarize their various functional consequences on the 3D structure of wildtype rH19-20 (Fig. 1*B*) and to infer that the wildtype residue is directly involved in ligand-binding if its substitution alters affinity. On this basis, Figure 1*B* illustrates that there is an overlapping binding patch on one face of module 20 for heparin and C3b. Two of the mutants that had minor or negligible effect on heparin binding (L1189F and V1197A, respectively) both involve conservative substitutions of buried side chains.

The rH19-20 aHUS-associated mutants are impaired in their ability to bind to C3b-coated host-like erythrocyte surfaces

A clear message of the results described above is that while ten mutants included in this study have been linked with occurrence of aHUS (48), not all of them are negatively affected in their ability to bind to C3b and polyanion ligands (summarized in Fig. 4). We therefore tested whether these mutations interfere with the ability of fH to bind, simultaneously, to C3b and host-like polyanions in a more physiological setting using a competitive binding assay, as previously described (35). In this assay, rH19-20 competes with radiolabeled full-length fH, inhibiting its binding to C3b and host-like polyanions on sheep erythrocytes (E_S), which carry high levels of sialic acid-containing polysaccharides (33, 34) (as do most human cells and tissues). We showed previously that such competition impairs fH complement-regulatory functions and increases complement activation on host surfaces (35). Thus, the C-terminal module-pair is important for anchoring fH to self-

surfaces following C3b deposition. Data in Figure 5*A* confirms that wildtype-sequence rH19-20 inhibits, in a dose dependent manner, the binding of full-length fH to C3b-coated host-like cells, with an IC_{50} of 0.2 μM. The aHUS-linked mutant forms of rH19-20, on the other hand, were significantly impaired in their ability to compete, displaying from < 2.5% (R1215G, D1119G and R1182S) to 40-50% (T1184R and R1210C) of the inhibitory activity of the wildtype rH19-20 (Fig. 5*A*). Only the designed mutant (E1172R) retained more than 70% activity in this assay. The presence of the V1197A mutation within the double mutant S1191L;V1197A did not further impair its ability to compete *versus* S1191L alone.

We also determined the effect of the mutations on the ability of rH19-20 to compete with radiolabeled wildtype rH19-20, *i.e.* without the potential interference of the other C3b/polyanion-binding sites or higher-order architecture of full-length fH, and very similar results were obtained (Fig. 5*B*). Thus, the four aHUS mutants that were most affected (D1119G, R1182S, W1183R, and R1215G) and the two least affected mutants (T1184R and R1210C) in the competition assay with full-length ^{125}I-fH, ranked comparably in the competition assay with ^{125}I-rH19-20, and can be compared in summary Figure 4.

Ability of rH19-20 aHUS-associated mutants to inhibit fH-mediated protection of human erythrocytes from complement-mediated lysis

Experiments were performed in which complement-mediated lysis of human erythrocytes was measured in the presence of normal human serum and rH19-20 mutants (Fig. 6). Wildtype rH19-20 competes with fH, inhibiting fH-mediated protective action more effectively than any of the aHUS-linked mutants, apart from R1210C and T1184R, which are comparably effective. This is largely consistent with the cell-surface binding results (Fig. 5) and provides further evidence that anchoring of fH to self-surfaces via its C-terminus is essential for its protective function.

Thus, the competition data strongly indicate that a common feature of aHUS-linked fH mutants is the reduced ability to engage, in a functionally effective way, with the fH target (C3b/C3d), when in the context of polyanion-rich self-surfaces. Intriguingly, this behavior on physiological cell surfaces does not correlate with the increased affinity that some of the aHUS mutants displayed for C3b (Fig. 3) and/or for the GAG-model compound heparin (Fig. 2), when these interactions were analyzed individually.

Discussion

If a mutation were to impair the ability of fH to regulate complement at self-surfaces it would have particularly significant consequences for tissue and cell surfaces thought to rely on fH for protection from complement-mediated damage. An example is the glomerular basement membrane that lacks membrane-bound complement regulators, but is exposed to plasma (and therefore the alternative pathway of complement), by fenestrations between the endothelial cells of the glomerular microvasculature. Thus, fH mutations clustered within the surface-anchoring C-terminal region, which have been detected in a significant proportion of aHUS patients, may be expected to directly trigger or exacerbate pathogenesis. Understanding the precise properties of disease-linked mutants of fH will therefore help to clarify the molecular basis of aHUS. For example, disease-associated mutations in the C-terminal region may disrupt its three-dimensional protein structure. Alternatively, they could interfere with the recognition site in CCP 20 of fH for polyanionic self markers, or they may perturb the C-terminal binding site for surface-bound C3b, or they could affect both polyanion and C3b-binding sites simultaneously. In the present study, we sought to distinguish between these various possibilities.

Our NMR analyses show that none of the ten disease-linked mutations in the current study result in anything other than highly localized effects on the structures of CCPs 19 or 20. Consequently, any functional effects of these mutations may reasonably be ascribed to their location within, or near to, critical binding sites on the wildtype protein. C3b- and heparin-binding data collected on these and five further, structurally intact, “designer” mutations in the context of rH19-20 allow the most comprehensive delineation of binding sites for these ligands to date. This exercise (summarized in Figs. 1*B* and 4) suggests that positively charged binding sites for heparin and C3b overlap on one face of rH19-20. The binding surface for heparin (and by extension, for other glycosaminoglycans) appears to extend towards the C-terminus of fH while the C3b-binding surface extends into module 19. Changes in the electrostatic nature of the surface had the largest influences (gain of positive charge or loss of negative charge appeared to correlate with increases of both heparin and C3b-binding), thus it is possible that some of the residues concerned are involved in electrostatic steering effects rather than direct contacts with ligands. These findings are in partial agreement with previous reports (40, 41) but do not support a suggestion of simultaneously occupied binding sites on opposite faces of CCP 20 (41).

Functional analyses of some aHUS-associated mutants reveal effects consistent with an intuitively feasible model of aHUS pathogenesis; *i.e.* their reduced ability to bind to a polyanion-rich C3b-coated host-like surface correlates with their diminished performance in assays that measure directly affinity for C3b or for heparin. For example, although D1119G (involving loss of a negative charge) is unaffected in its ability to bind heparin, it has significantly diminished affinity for C3b (Fig. 3-4) and this mutant was also the weakest of all the mutants in the cell surface assays. Moreover, analysis of some of the “designer” mutants (*i.e.* those engineered for this study to help delineate C3b- and heparin- binding sites, but not identified in any aHUS patients to date) also produced results that appear to link an affinity for C3b and/or heparin to a capacity for blocking fH binding to a C3b-coated erythrocyte surface. Thus, the designer mutant R1210S binds C3b with wildtype affinity and is only slightly diminished in affinity for heparin, while maintaining near-wildtype activity in the cell surface assay. The case of the aHUS-linked R1210C is complicated by the likelihood that it forms disulfide bonds with itself or other proteins (54) (recombinant R1210C was found to be glutathionylated in our study). In all, seven mutations (aHUS-linked mutants R1215G and R1182S, and designer mutants K1188Q, R1203S, R1210S, K1230A) display both weaker heparin and C3b binding (Figs. 2-3) and, as expected, their performance is significantly impaired in the cell-surface assays (Fig. 5). It should be noted that the reduced heparin binding obtained with R1182S contrasts with the unaffected heparin binding previously observed with a mutant, R1182A, which has not been found in aHUS patients (40).

Indeed all the aHUS-associated mutants exhibit a weaker than wildtype ability to compete with fH for erythrocyte surface binding (Fig. 5). For example, L1189R and W1183R perform very poorly in cell-surface assays (Fig. 5-6), while T1184R and R1210C are the only aHUS-mutants that are nearly as good at inhibiting the protective effects of fH as the wildtype rH19-20. What is striking is that several of these mutations have a higher affinity both for heparin (Figs. 2 and 4) and for C3b (Fig. 3-4). Such is the case for aHUS mutants W1183R, T1184R, L1189R, and the designer mutation E1172R, all of which involve an introduction of one or more positive charges. Note that in the case of the W1183R mutant, the observed increased affinity for C3b and heparin differed from what had been observed previously with another aHUS-linked mutant, W1183L (40) that had reduced binding to C3b and heparin; unlike W1183L (40), the W1183R mutant ran as a single band by SDS-PAGE (not shown). The L1189F mutation also shows increased C3b- and heparin-binding, albeit to a much lesser extent than L1189R (Figs. 3-4). Another mutant (S1191L) with weaker than wildtype activity in the cell surface assays (Figs. 5-6), has enhanced affinity for C3b (Fig.

3), contrary to previously reported results (54, 55). This same mutant had no effect on heparin binding (Fig. 2), in agreement with a previous study (55). Interestingly, the presence of V1197A in the S1191L;V1197A double mutant has no additional effect in any of the assays tested *versus* the S1191L mutant.

An overall summary of the heparin and C3b binding results (where a wide range of affinities for C3b and heparin were observed), and the cell-surface complement functional assays (where all aHUS-linked mutants were impaired), is illustrated in Figure 4. Taken together these results unexpectedly show that, measured separately, affinities for C3b and heparin do not correlate consistently with the strength of binding to a polyanion-rich erythrocyte surface (on which C3b has been deposited); nor do they correlate with the disease-risk phenotype.

In the case of heparin it is conceivable that this material is not in fact representative of a putative host tissue-specific polyanionic ligand. The presence in such a ligand of particular patterns or densities of sulfation, for example, might result in differential binding amongst the mutants that correlates better with cell-surface assays. Studies aimed at identifying physiological polyanion species, as well as elucidating their chemical nature, are warranted.

The lack of correlation between the separate ligand binding assays and the cell based assays also suggests that a mutation may affect a third functional site in CCPs 19-20, perhaps different from those involved in C3b or polyanion binding. For example, a mutation could affect the region involved in the formation of putative dimers or tetramers (40, 56-58), which may be important for fH binding/function on the cell surface. In this regard, we have recently determined that polyanions greatly promote formation of fH dimers and tetramers, and that this dimerization/tetramerization leads to an increase in fH binding and complement control activity at the cell surface (58). In addition, we have determined that this polyanion-induced self-assembly is mediated, at least in part, by C-terminus to C-terminus complex formation, specifically through CCP 18-20 (58).

A further possibility derives from consideration of the relative affinities of fH for each ligand in the setting of the cell surface, and the order of binding events. An increased affinity between fH and polyanions, due to CCP 19-20 mutations, may result in a decrease in the ability of fH to diffuse normally over the cell surface, impairing its ability to efficiently encounter and bind C3b. Thus, such mutants would be less effective than normal CCP 19-20 that binds with the correct affinity to the combination of both ligands (polyanions and C3b/C3d). Likewise, the mutants that were found to have increased affinity for C3b may get retained/delayed in complexes with the products of decay acceleration and cofactor activity (*i.e.* C3b/iC3b).

Thus, we propose that aHUS-linked mutations disturb a complex relationship between affinities of fH for its individual ligands (C3b and physiological polyanions) or possibly for itself, in the context of the cell surface.

Acknowledgments

The authors express their appreciation to Connie Elliot for her excellent technical assistance and to Dr. Pierre Neuenschwander for helpful advice on operation of the BIAcore 3000 instrument.

The abbreviations used are

fH	factor H
aHUS	atypical hemolytic uremic syndrome

CCP	complement control protein domain
rH 19-20	recombinant domains 19-20 of factor H
GAG	glycosaminoglycans
VBS	Veronal-buffered saline
GVB	VBS containing 0.1% gelatin
GVBE	GVB containing 10 mM EDTA
MgEGTA	equimolar $MgCl_2$ and EGTA
NHS	normal human serum
GMSA	gel mobility shift assay
dp6	hexasaccharide
SPR	surface plasmon resonance
RU	response unit
E_H	human erythrocytes
E_SC3b	C3b-coated erythrocytes

References

1. Kavanagh D, Richards A, Atkinson J. Complement regulatory genes and hemolytic uremic syndromes. Annu. Rev. Med. 2008; 59:293–309. [PubMed: 17705684]
2. Warwicker P, Goodship TH, Donne RL, Pirson Y, Nicholls A, Ward RM, Turnpenny P, Goodship JA. Genetic studies into inherited and sporadic hemolytic uremic syndrome. Kidney Int. 1998; 53:836–844. [PubMed: 9551389]
3. Perez-Caballero D, Gonzalez-Rubio C, Gallardo ME, Vera M, Lopez-Trascasa M, Rodriguez de Cordoba S, Sanchez-Corral P. Clustering of missense mutations in the C-terminal region of factor H in atypical hemolytic uremic syndrome. Am. J. Hum. Genet. 2001; 68:478–484. [PubMed: 11170895]
4. Richards A, Buddles MRH, Donne RL, Kaplan BS, Kirk E, Venning MC, Tielemans CL, Goodship JA, Goodship TH. Factor H mutations in hemolytic uremic syndrome cluster in exons 18-20, a domain important for host cell recognition. Am. J. Hum. Genet. 2001; 68:485–490. [PubMed: 11170896]
5. Dragon-Durey MA, Fremeaux-Bacchi V, Loirat C, Blouin J, Niaudet P, Deschenes G, Coppo P, Herman FW, Weiss L. Heterozygous and homozygous factor H deficiencies associated with hemolytic uremic syndrome or membranoproliferative glomerulonephritis: report and genetic analysis of 16 cases. J. Am. Soc. Nephrol. 2004; 15:787–795. [PubMed: 14978182]
6. Neumann HP, Salzmann M, Bohnert-Iwan B, Mannuelian T, Skerka C, Lenk D, Bender BU, Cybulla M, Riegler P, Konigsrainer A, Neyer U, Bock A, Widmer U, Male DA, Franke G, Zipfel PF. Haemolytic uraemic syndrome and mutations of the factor H gene: a registry-based study of German speaking countries. J. Med. Genet. 2003; 40:676–681. [PubMed: 12960213]
7. Caprioli J, Bettinaglio P, Zipfel PF, Amadei B, Daina E, Gamba S, Skerka C, Marziliano N, Remuzzi G, Noris M. The molecular basis of familial hemolytic uremic syndrome: mutation analysis of factor H gene reveals a hot spot in short consensus repeat 20. J. Am. Soc. Nephrol. 2001; 12:297–307. [PubMed: 11158219]
8. Esparza-Gordillo J, Goicoechea de JE, Buil A, Carreras BL, Lopez-Trascasa M, Sanchez-Corral P, Rodriguez de CS. Predisposition to atypical hemolytic uremic syndrome involves the concurrence of different susceptibility alleles in the regulators of complement activation gene cluster in 1q32. Hum. Mol. Genet. 2005; 14:703–712. [PubMed: 15661753]

9. Esparza-Gordillo J, Jorge EG, Garrido CA, Carreras L, Lopez-Trascasa M, Sanchez-Corral P, de C Sr. Insights into hemolytic uremic syndrome: Segregation of three independent predisposition factors in a large, multiple affected pedigree. Mol. Immunol. 2006; 43:1769–1775. [PubMed: 16386793]
10. Caprioli J, Noris M, Brioschi S, Pianetti G, Castelletti F, Bettinaglio P, Mele C, Bresin E, Cassis L, Gamba S, Porrati F, Bucchioni S, Monteferrante G, Fang CJ, Liszewski MK, Kavanagh D, Atkinson JP, Remuzzi G. Genetics of HUS: the impact of MCP, CFH, and IF mutations on clinical presentation, response to treatment, and outcome. Blood. 2006; 108:1267–1279. [PubMed: 16621965]
11. Caprioli J, Castelletti F, Bucchioni S, Bettinaglio P, Bresin E, Pianetti G, Gamba S, Brioschi S, Daina E, Remuzzi G, Noris M. Complement factor H mutations and gene polymorphisms in haemolytic uraemic syndrome: the C-257T, the A2089G and the G2881T polymorphisms are strongly associated with the disease. Hum. Mol. Genet. 2003; 12:3385–3395. [PubMed: 14583443]
12. Fremeaux-Bacchi V, Kemp EJ, Goodship JA, Dragon-Durey MA, Strain L, Loirat C, Deng HW, Goodship TH. The development of atypical haemolytic-uraemic syndrome is influenced by susceptibility factors in factor H and membrane cofactor protein: evidence from two independent cohorts. J. Med. Genet. 2005; 42:852–856. [PubMed: 15784724]
13. Pangburn MK. Differences between the binding sites of the complement regulatory proteins DAF, CR1 and Factor H on C3 convertases. J. Immunol. 1986; 136:2216–2221. [PubMed: 2419425]
14. Harrison RA, Lachmann PJ. The physiological breakdown of the third component of human complement. Mol. Immunol. 1980; 17:9–20. [PubMed: 7360115]
15. Discipio RG. Ultrastructures and interactions of complement factors H and I. J. Immunol. 1992; 149:2592–2599. [PubMed: 1401896]
16. Moore MD, Discipio RG, Cooper NR, Nemerow GR. Hydrodynamic, electron microscopic, and ligand-binding analysis of the Epstein-Barr virus/C3dg receptor (CR2). J. Biol. Chem. 1989; 264:20576–20582. [PubMed: 2555366]
17. Alsenz J, Lambris JD, Schulz TF, Dierich MP. Localization of the complement component C3b binding site and the cofactor activity for factor I in the 38 kDa tryptic fragment of factor H. Biochem. J. 1984; 224:389–398. [PubMed: 6240261]
18. Gordon DL, Kaufman RM, Blackmore TK, Kwong J, Lublin DM. Identification of complement regulatory domains in human factor H. J. Immunol. 1995; 155:348–356. [PubMed: 7541419]
19. Kuhn S, Zipfel PF. Mapping of the domains required for decay acceleration activity of the human factor H-like protein 1 and factor H. Eur. J. Immunol. 1996; 26:2383–2387. [PubMed: 8898949]
20. Kühn S, Skerka C, Zipfel PF. Mapping of the complement regulatory domains in the human factor H-like protein 1 and in factor H. J. Immunol. 1995; 155:5663–5670. [PubMed: 7499851]
21. Jokiranta TS, Hellwage J, Koistinen V, Zipfel PF, Meri S. Each of the three binding sites on factor H interacts with a distinct site on C3b. J. Biol. Chem. 2000; 275:27657–27662. [PubMed: 10837479]
22. Pangburn MK, Shreedhar M, Alam N, Rawal N, Herbert A, Haque A. Functional analysis of each of the three C3b binding sites of factor H and comparison with full length factor H [abstract]. Mol. Immunol. 2004; 41:291.
23. Sharma AK, Pangburn MK. Identification of three physically and functionally distinct binding sites for C3b in human complement factor H by deletion mutagenesis. Proc. Natl. Acad. Sci. USA. 1996; 93:10996–11001. [PubMed: 8855297]
24. Blackmore TK, Sadlon TA, Ward HM, Lublin DM, Gordon DL. Identification of a heparin binding domain in the seventh short consensus repeat of complement factor H. J. Immunol. 1996; 157:5422–5427. [PubMed: 8955190]
25. Blackmore TK, Hellwage J, Sadlon TA, Higgs N, Zipfel PF, Ward HM, Gordon DL. Identification of the second heparin-binding domain in human complement factor H. J. Immunol. 1998; 160:3342–3348. [PubMed: 9531293]
26. Pangburn MK, Atkinson MAL, Meri S. Localization of the heparin-binding site on complement factor H. J. Biol. Chem. 1991; 266:16847–16853. [PubMed: 1832158]

27. Prodinger WM, Hellwage J, Spruth M, Dierich MP, Zipfel PF. The C-terminus of factor H: monoclonal antibodies inhibit heparin binding and identify epitopes common to factor H and factor H-related proteins. Biochem. J. 1998; 331(Pt 1):41–47. [PubMed: 9512460]
28. Ram S, Sharma AK, Simpson SD, Gulati S, McQuillen DP, Pangburn MK, Rice PA. A novel sialic acid binding site on factor H mediates serum resistance of sialylated *Neisseria gonorrhoeae*. J. Exp. Med. 1998; 187:743–752. [PubMed: 9480984]
29. Schmidt CQ, Herbert AP, Kavanagh D, Gandy C, Fenton CJ, Blaum BS, Lyon M, Uhrin D, Barlow PN. A new map of glycosaminoglycan and C3b binding sites on factor H. J. Immunol. 2008; 181:2610–2619. [PubMed: 18684951]
30. Prosser BE, Johnson S, Roversi P, Herbert AP, Blaum BS, Tyrrell J, Jowitt TA, Clark SJ, Tarelli E, Uhrin D, Barlow PN, Sim RB, Day AJ, Lea SM. Structural basis for complement factor H linked age-related macular degeneration. J. Exp. Med. 2007; 204:2277–2283. [PubMed: 17893204]
31. Jokiranta TS, Cheng ZZ, Seeberger H, Jozsi M, Heinen S, Noris M, Remuzzi G, Ormsby R, Gordon DL, Meri S, Hellwage J, Zipfel PF. Binding of complement factor H to endothelial cells is mediated by the carboxy-terminal glycosaminoglycan binding site. Am. J. Pathol. 2005; 167:1173–1181. [PubMed: 16192651]
32. Pickering M, Cook H, Warren J, Bygrave A, Moss J, Walport MJ, Botto M. Uncontrolled C3 activation causes membranoproliferative glomerulonephritis in mice deficient in complement factor H. Nat. Genet. 2002; 31:424–428. [PubMed: 12091909]
33. Fearon DT. Regulation by membrane sialic acid of BIH-dependent decay-dissociation of amplification C3 convertase of the alternative complement pathway. Proc. Natl. Acad. Sci. USA. 1978; 75:1971–1975. [PubMed: 273923]
34. Pangburn MK, Muller-Eberhard HJ. Complement C3 convertase: cell surface restriction of BIH control and generation of restriction on neuraminidase treated cells. Proc. Natl. Acad. Sci. USA. 1978; 75:2416–2420. [PubMed: 276881]
35. Ferreira VP, Herbert AP, Hocking HG, Barlow PN, Pangburn MK. Critical role of the C-terminal domains of factor H in regulating complement activation at cell surfaces. J. Immunol. 2006; 177:6308–6316. [PubMed: 17056561]
36. Jozsi M, Oppermann M, Lambris JD, Zipfel PF. The C-terminus of complement factor H is essential for host cell protection. Mol. Immunol. 2007; 44:2697–2706. [PubMed: 17208302]
37. Pangburn MK. Cutting edge: Localization of the host recognition functions of complement factor H at the carboxyl-terminal: implications for hemolytic uremic syndrome. J. Immunol. 2002; 169:4702–4706. [PubMed: 12391176]
38. FH aHUS Mutation Database Version 2.1. R.E. Saunders and S.J. Perkins of the University College of London, UK, and The European Working Party on the Genetics of HUS; 2008. http://www.fh-hus.org/
39. Pickering MC, de Jorge EG, Martinez-Barricarte R, Recalde S, Garcia-Layana A, Rose KL, Moss J, Walport MJ, Cook HT, de C Sr. Botto M. Spontaneous hemolytic uremic syndrome triggered by complement factor H lacking surface recognition domains. J. Exp. Med. 2007; 204:1249–1256. [PubMed: 17517971]
40. Jokiranta TS, Jaakola VP, Lehtinen MJ, Parepalo M, Meri S, Goldman A. Structure of complement factor H carboxyl-terminus reveals molecular basis of atypical haemolytic uremic syndrome. EMBO J. 2006; 25:1784–1794. [PubMed: 16601698]
41. Herbert AP, Uhrin D, Lyon M, Pangburn MK, Barlow PN. Disease-associated sequence variations congregate in a polyanion-recognition patch on human factor H revealed in 3D structure. J. Biol. Chem. 2006; 281:16512–16520. [PubMed: 16533809]
42. Lecak J, Scott K, Young C, Hannon J, Acker JP. Evaluation of red blood cells stored at −80 degrees C in excess of 10 years. Transfusion. 2004; 44:1306–1313. [PubMed: 15318853]
43. Pangburn MK, Schreiber RD, Muller-Eberhard HJ. Human complement C3b inactivator: Isolation, characterization, and demonstration of an absolute requirement for the serum protein BIH for cleavage of C3b and C4b in solution. J. Exp. Med. 1977; 146:257–270. [PubMed: 301546]
44. Hammer CH, Wirtz GH, Renfer L, Gresham HD, Tack BF. Large scale isolation of functionally active components of the human complement system. J. Biol. Chem. 1981; 256:3995–4006. [PubMed: 6783652]

45. Pangburn MK. A fluorimetric assay for native C3. The hemolytically active form of the third component of human complement. J. Immunol. Methods. 1987; 102:7–14. [PubMed: 3624878]
46. Gotze O, Muller-Eberhard HJ. The C3-activator system: an alternative pathway of complement activation. J. Exp. Med. 1971; 134:90s–108s. [PubMed: 4105810]
47. Lesavre PH, Hugli TE, Esser AF, Muller-Eberhard HJ. The alternative pathway C3/C5 convertase: Chemical basis of factor B activation. J. Immunol. 1979; 123:529–534. [PubMed: 458145]
48. Kavanagh D, Goodship TH, Richards A. Atypical haemolytic uraemic syndrome. Br. Med. Bull. 2006; 77-78:5–22. [PubMed: 16968692]
49. Expert Protein Analysis System (EXPASY) proteomics server of the Swiss Institute of Bioinformatics. ProtParam tool. 2008http://www.expasy.org/tools/protparam.html
50. Lyon M, Deakin JA, Lietha D, Gherardi E, Gallagher JT. The interactions of hepatocyte growth factor/scatter factor and its NK1 and NK2 variants with glycosaminoglycans using a modified gel mobility shift assay. Elucidation of the minimal size of binding and activatory oligosaccharides. J. Biol. Chem. 2004; 279:43560–43567. [PubMed: 15292253]
51. Catlow KR, Deakin JA, Wei Z, Delehedde M, Fernig DG, Gherardi E, Gallagher JT, Pavao MS, Lyon M. Interactions of hepatocyte growth factor/scatter factor with various glycosaminoglycans reveal an important interplay between the presence of iduronate and sulfate density. J. Biol. Chem. 2008; 283:5235–5248. [PubMed: 18156180]
52. Mitchell DA, Ilyas R, Dodds AW, Sim RB. Enzyme-independent, orientation-selective conjugation of whole human complement C3 to protein surfaces. J. Immunol. Methods. 2008; 337:49–54. [PubMed: 18572187]
53. Rawal N, Pangburn MK. C5 convertase of the alternative pathway of complement. Kinetic analysis of the free and surface-bound forms of the enzyme. J. Biol. Chem. 1998; 273:16828–16835. [PubMed: 9642242]
54. Sanchez-Corral P, Perez-Caballero D, Huarte O, Simckes AM, Goicoechea E, Lopez-Trascasa M, Rodriguez de Cordoba S. Structural and functional characterization of factor H mutations associated with atypical hemolytic uremic syndrome. Am. J. Hum. Genet. 2002; 71:1285–1295. [PubMed: 12424708]
55. Heinen S, Sanchez-Corral P, Jackson MS, Strain L, Goodship JA, Kemp EJ, Skerka C, Jokiranta TS, Meyers K, Wagner E, Robitaille P, Esparza-Gordillo J, Rodriguez de CS, Zipfel PF, Goodship TH. De novo gene conversion in the RCA gene cluster (1q32) causes mutations in complement factor H associated with atypical hemolytic uremic syndrome. Hum. Mutat. 2006; 27:292–293. [PubMed: 16470555]
56. Nan R, Gor J, Perkins SJ. Implications of the progressive self-association of wild-type human factor H for complement regulation and disease. J. Mol. Biol. 2008; 375:891–900. [PubMed: 18054958]
57. Okemefuna AI, Gilbert HE, Griggs KM, Ormsby RJ, Gordon DL, Perkins SJ. The regulatory SCR-1/5 and cell surface-binding SCR-16/20 fragments of factor H reveal partially folded-back solution structures and different self-associative properties. J. Mol. Biol. 2008; 375:80–101. [PubMed: 18005991]
58. Pangburn MK, Rawal N, Cortes C, Alam MN, Ferreira VP, Atkinson MA. Polyanion-induced self-association of complement factor H. J. Immunol. 2009; 182:1061–1068. [PubMed: 19124749]

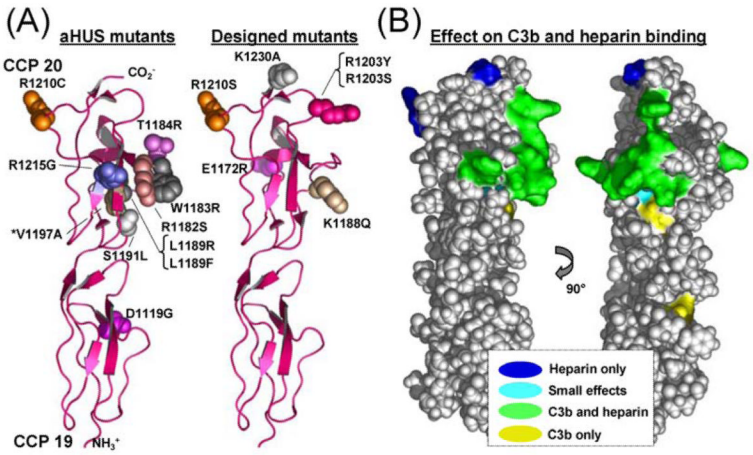

FIGURE 1.

Summary of mutagenesis study mapped onto 3-D structure of fH CCP 19-20. *A*, Side-chain heavy atoms of disease-linked mutations (left-hand panel) or non-disease linked mutations are drawn (in various colors for clarity) on cartoon representations of fH CCP 19-20. *V1197A was made in the context of the double mutant - V1197A;S1191L. *B*, A surface representation of mutated residues is superimposed on the structure (orthogonal views are shown; left-hand view is identical to that in *A*) and color-coded (see key) according to the predominant impact of the mutation on ligand binding. Positive and negative effects were not discriminated - “Heparin only” implies that the effect on C3b-binding was small while “C3b only” implies a small effect on heparin binding. The cyan color indicating “small effect” refers to that of L1189F on C3b and heparin binding. L1189R had significantly increased binding to both C3b and heparin.

Europe PMC Funders Author Manuscripts

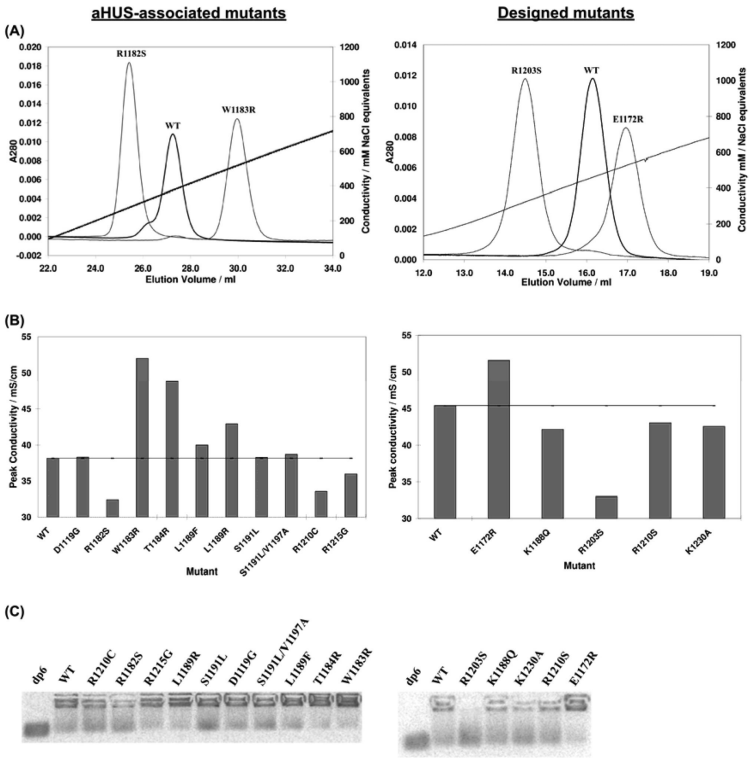

FIGURE 2.

Affinities of wildtype and mutant rH19-20 for glycosaminoglycans. Variants of rH19-20 were eluted from a HiTrap heparin-affinity chromatography column and protein elution was monitored using absorbance at 280 nm (*A*). In (*A*), left panel, for clarity, only the elution profile of the aHUS-associated mutant with the highest (W1183R) and the lowest (R1182S) affinity for heparin are shown in comparison to wildtype rH19-20. The conductivity values at which the aHUS-associated mutants eluted are summarized in (*B*), left panel. In (*A*), right panel, only the elution profile of the designed mutant with the highest (E1172R) and the lowest (R1203S) affinity for heparin are shown in comparison to wildtype rH19-20. The conductivity values at which all the designed mutants eluted are shown in (*B*), right panel. *C*, GMSA results. For these assays, 2-aminoacridone-tagged heparin-derived hexasaccharides were combined with rH19-20 or its mutants to give 34 μM protein and 40 μM oligosaccharide in 12 μl PBS containing 5 mM EDTA. To these samples were added 0.5 μl of glycerol and a trace of phenol red before incubation (15 minutes, room temperature). Samples were then loaded on a 1% agarose gel in 10 mM Tris-HCl, pH 7.4, and 1 mM EDTA. Electrophoresis was performed (120 mV, 5 min) in a horizontal agarose electrophoresis system, using an electrophoresis buffer (40 mM Tris/acetate, 1 mM EDTA, pH 7.4). Immediately thereafter, the fluorescent oligosaccharides were visualized. The left and right-hand panels show the data obtained with the aHUS-associated mutants or the designed mutants, respectively. All results are representative of two separate experiments.

Europe PMC Funders Author Manuscripts

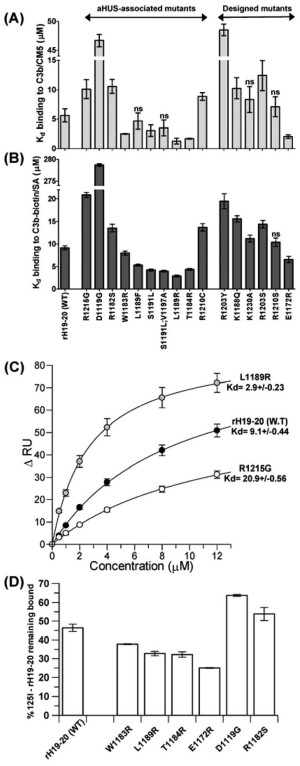

FIGURE 3.

Binding affinity of the rH19-20 mutants for C3b. *A*, K_d values for the binding of rH19-20 to C3b were measured on a CM5 sensor chip using surface plasmon resonance. Assays were performed on a BIAcore 3000 instrument by immobilizing 800-2000 response units (RU) of human C3b to three independent flow cells of a CM5 chip, using amine coupling. The rH19-20 mutants or wildtype rH19-20 were injected at 0-12 μM over the flow cells. The maximum equilibrium binding, at each concentration, was plotted using the Grafit 5 program, which determined the apparent K_d by fitting the data to a single-site saturation curve, where the capacity was fixed (as a constant) to that of the average (n=12) wildtype rH19-20 capacity. The standard deviations correspond to the K_d values obtained when samples were injected over the three different C3b-coated flow cells. *B*, Same as panel *A*, except biotinylated C3b was used to coat a streptavidin sensor chip. The non-significant (n.s.) differences between the ability of the wildtype rH19-20 versus each of the mutants to bind to C3b ($p>0.05$) are indicated. *C*, Representative equilibrium C3b-biotin binding curves for rH19-20 wildtype as well as a high binding (L1189R) and a low binding (R1215G) mutant. *D*, Analysis of the ability of rH19-20 mutants to compete with radiolabeled wildtype rH19-20 for binding to C3b on zymosan particles. Zymosan particles bearing 1 μg C3b were incubated with ~20 ng ^{125}I-rH19-20 (wildtype) in combination with the IC_{50} dose of unlabeled wildtype rH19-20 (1.5 μM) or with 1.5 μM of the rH19-20 mutants in 100 μl DGVB. After 20 min at 22°C, the bound and free radiolabel were separated by centrifugation of cells through 20% sucrose in DGVB. The average (n=4) percent of ^{125}I-rH19-20 remaining bound to the zymosan-C3b (ZymC3b) and standard deviations are shown for each protein. The differences between the ability of the wildtype versus each of the mutants to bind to ZymC3b were all significant ($p<0.05$). The results shown are from one of two representative experiments.

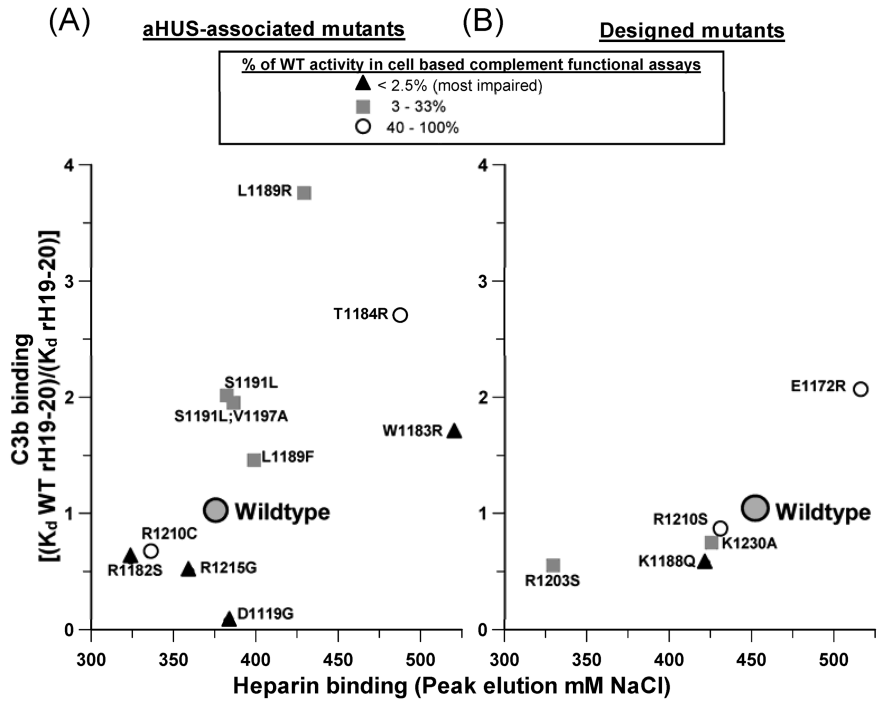

FIGURE 4.

Summary figure of relative affinities of rH19-20 wildtype and mutant proteins for C3b and heparin, and of complement functional cell-based assays. The salt concentration (mM NaCl) at which the rH19-20 wildtype or mutant proteins eluted from the heparin affinity column are graphed on the x-axis. The relative affinity of the mutants *versus* the wildtype (WT) protein for C3b is graphed on the y-axis using the formula: relative affinity = [(K_d of WT rH19-20) / (K_d of each rH19-20 mutant)]. The average of the K_d values obtained on the C3b-coated CM5 and SA sensor chips were used. The higher values represent higher affinity for each ligand, while lower values represent the opposite. The symbols that represent each mutant depend on their % of remaining wildtype activity in the cell-based assay that measured the ability of the mutants to inhibit fH binding to C3b-coated host-like cells (Fig. 5*A*). These values are in agreement with the results obtained in the E_H lysis assay (Fig. 6).

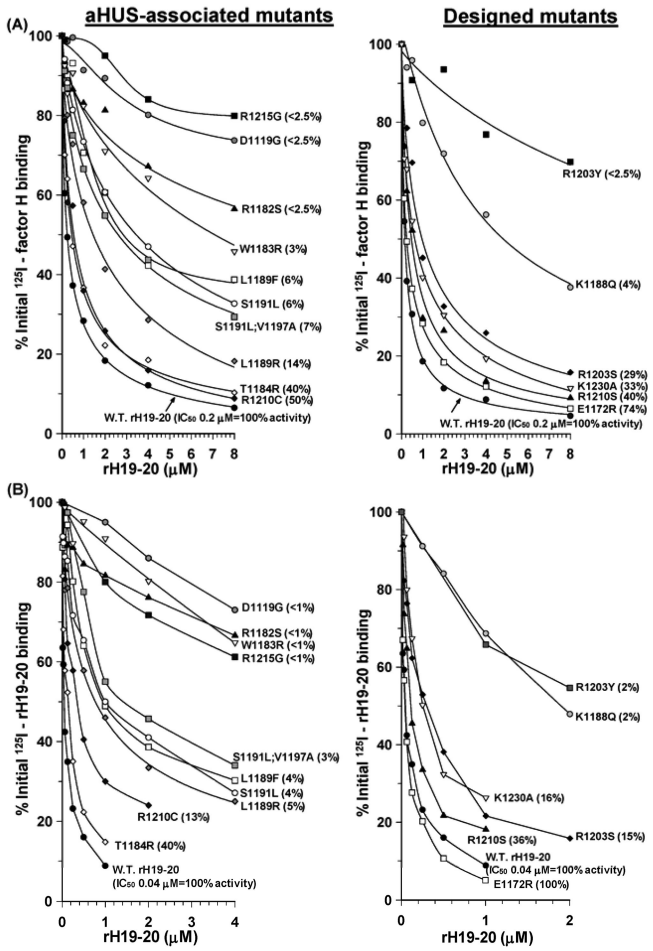

FIGURE 5.

The rH19-20 mutants are impaired in their ability to bind to C3b-coated host-like erythrocyte surfaces. *A*, Binding of radiolabeled fH to C3b on E_SC3b cells in the presence of unlabeled wildtype or mutant rH19-20. Cells bearing 34×10^{11} C3b (1 μg) were incubated with ~ 20 ng of radioiodinated human fH and 0 to 8 μM of non-labeled wildtype or mutant rH19-20, in 100 μl DGVB. After 20 min at 22°C, the bound and free radiolabel were separated by centrifugation of cells through 20% sucrose in DGVB. The results are graphed relative to the initial binding observed with labeled fH in the absence of the rH19-20 proteins. Each experiment was carried out with five proteins at a time, using wildtype rH19-20 as an internal control in each set of assays. The average (n=5) wildtype rH19-20 IC_{50} is shown and was 0.20 +/− 0.04. The percent of inhibitory activity remaining for each protein is shown in parenthesis and was calculated using the following formula: (IC_{50} wildtype rH19-20 / IC_{50} mutant rH19-20) × 100. *B*, Same as above, except the C3b-coated cells were incubated with radioiodinated rH19-20 instead. The average wildtype (n=3) rH19-20 IC_{50} was 0.04 +/− 0.01. The left and right-hand panels in *A*-*B* show the data obtained with the aHUS-associated mutants or the designed mutants, respectively.

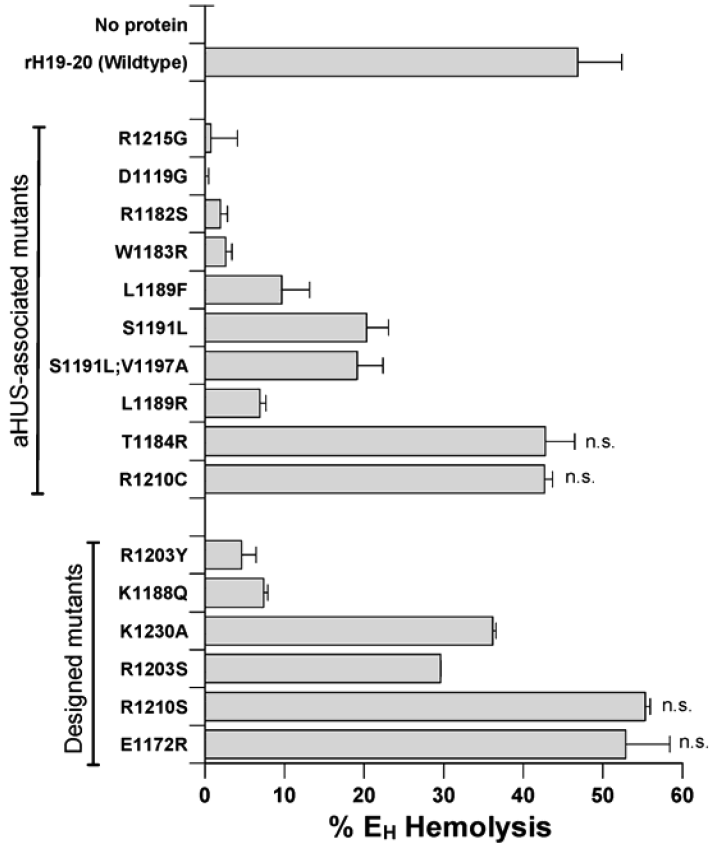

FIGURE 6.

Ability of rH19-20 mutants to inhibit fH-mediated protection of human erythrocytes from complement-mediated lysis. Lysis of human erythrocytes (E_H) was measured by pre-incubating anti-CD59-treated E_H (5×10^6) with 1 μM wildtype or mutant rH19-20, in the presence of 40% NHS. This concentration of wildtype rH19-20 is enough to achieve ~ 50% hemolysis (IC_{50}) of anti-CD59-treated cells, due to inhibition (by rH19-20) of fH-mediated protection. The mixture was incubated for 20 min, at 37°C. To determine the extent of hemolysis induced by the mutants *versus* the wildtype rH19-20, 200 μl cold GVBE was added, the samples were centrifuged and the optical density of the supernatant was determined at 414 nm. The percentage of lysis is graphed by subtracting the A_{414} of the background lysis control, as well as the percentage of lysis induced by blocking CD59 alone (~20%), and dividing this value by the maximum lysis obtained with water. The non-significant (n.s.) differences between the ability of the wildtype rH19-20 *versus* each of the mutants to induce lysis of E_H ($p>0.05$) are indicated. The results are representative of two separate experiments shown as means and standard deviations of triplicate observations.